FIELD LOAD TEST AND GIRDER DISTRIBUTION FACTORS OF MISSOURI BRIDGE A7957

Eli S. Hernandez, PhD Candidate, Department of Civil, Architectural and Environmental Engineering, Missouri University of Science and Technology, Rolla, MO
John J. Myers, PhD, PE, Department of Civil, Architectural and Environmental Engineering, Missouri University of Science and Technology, Rolla, MO

ABSTRACT

Self-consolidating concrete (SCC) has become widely accepted because of its inherent benefits including a higher construction and cost effectiveness compared to traditional concrete mixtures. Innovative materials such as high volume fly ash concrete (HVFAC) also represents a remarkable progress to producing stronger and more durable cast-in-place (CIP) concrete elements. Bridge A7957 is the first large-scale structure employing both types of materials conducted by the Missouri Department of Transportation (MoDOT). The objective of this research was to perform an in-situ evaluation of Bridge A7957 to establish its baseline response. To fulfill this goal, Bridge A7957 was instrumented at critical locations with embedded vibrating wire strain gauges (VWSGs) to monitor and compare the precast prestressed girders' response from casting through service life. A field load test strategy was elaborated and carried out to evaluate the bridge's response under different static load configurations. During the load test, VWSGs recorded strain variations at different instrumented sections. Based on field results, lateral load distribution factors were obtained from recorded data and with the AASHTO LRFD Bridge Design Specifications. The load distribution factors estimated from the AASHTO LRFD approach resulted in larger values compared to the measured load distribution values.

Keywords: Girder distribution factors, GDF, HVFAC, Lateral load distribution, Self-consolidated concrete, SCC.

INTRODUCTION

Despite the benefits that come with using high-strength self-consolidating concrete (HS-SCC), there are some concerns related to its structural performance because of its constituent materials and proportions. Of particular interest is the effect of the larger paste content and the smaller coarse aggregate size employed in the concrete mixture[1]. It is critical to monitor the effects of using HS-SCC by examining the serviceability response of full-scale structures subjected to varying loads. As an attempt to investigate the serviceability and structural performance both short-term and long-term of the PC/PS concrete members of Bridge A7957, an instrumentation program was designed and implemented. Part of the instrumentation program consists of monitoring the PC/PS girders' strain values by conducting several series of field load tests during the service life of the structure.

The AASHTO LRFD Bridge Design Specifications[2] propose a design methodology that consists of determining what percentage of live load applied to a bridge is carried by each girder. The fraction of load carried by each element is defined as the lateral load distribution factor. Load distribution factors help convert a three-dimensional (3D) structural analysis into an equivalent one-dimensional (1D) structural analysis which is easier to handle by designers[3]. A live load effect (i.e., bending moment or shear force) is multiplied by a distribution factor and an estimation of the load effect carried by a longitudinal supporting member is performed. It is important to recall that the AASHTO LRFD does not propose a method to estimate how a load is distributed among the girders for in-service assessments of bridges. Instead, this approach proposes a methodology that conservatively estimates distribution factors used for design. Live load tests are used to assess the in-service lateral load distribution by directly considering field factors that favorably or adversely affect the response of a bridge structure[4]. In this research, a comparison between load factors obtained from field strain measurements and the AASHTO LRFD method was performed as an attempt to evaluate some of the differences between both methods.

BRIDGE DESCRIPTION

Bridge A7957 was built during the summer and fall of 2013. This bridge spans the Maries River and is located in Osage County, west of Linn, Missouri. The bridge is a three-span, continuous, PC/PS concrete bridge (Fig. 1). The PC/PS concrete NU53 girders (Fig. 1b) in each span were designed with different concrete mixtures[5]. Girders in the first span are 30.48 m (100 ft.) long and were made of conventional concrete (MoDOT's Class A-1 mixture) with a specified compressive strength of 55.2 MPa (8,000 psi). Girders in the second span are 36.58 m (120 ft.) and were fabricated with a HS-SCC mixture of 68.9 MPa (10,000 psi).
The girders in the third span are 30.48 m (100 ft.) long and were made of SCC with a design compressive strength of 55.2 MPa (8,000 psi). PC/PS concrete panels, with a specified compressive strength of 41.4 MPa (6,000 psi), extend between the top flanges of the girders in the transverse direction and underneath a CIP RC deck (Fig. 1b).

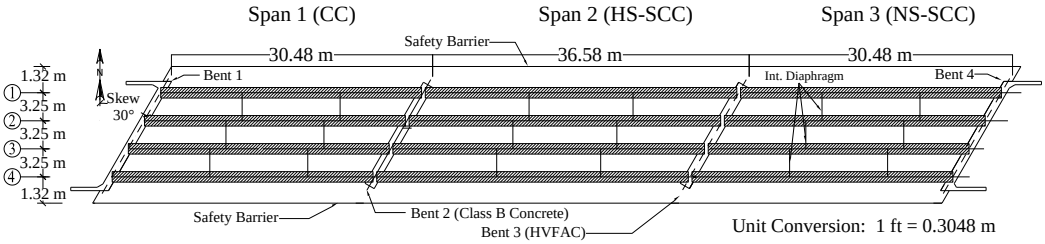

(a) Plan view

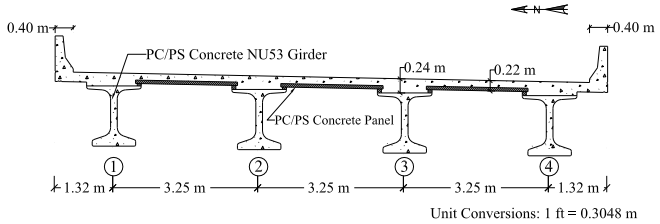

(b) Cross section

Fig. 1. Bridge A7957 details

The CIP deck was cast with a concrete mixture (MoDOT's modified Class B-2) using a 25 % fly ash replacement of portland cement whose target compressive strength was specified as 27.6 MPa (4,000 psi). Two intermediate bents and two abutments support the superstructure (Fig. 1a). The abutments and intermediate bent 2 were built with a mixture having a 20% fly ash replacement of portland cement. This concrete mixture is a MoDOT's class B concrete with a target compressive strength of 20.7 MPa (3,000 psi). Intermediate bent 3 was cast using HVFAC with a 50% fly ash replacement of portland cement designed with a specified compressive strength of 20.7 MPa (3,000 psi). As illustrated in Fig. 1a, the bridge is skewed 30 degrees.

BRIDGE INSTRUMENTATION

During the preconstruction of Bridge A7957, structural elements that were instrumented included: two PC/PS NU53 girders per span and two PC/PS panels located at mid-span. These two instrumented PC/PS panels were set in span 2, between girder lines 2 and 3, and girder lines 3 and 4, respectively. The type of sensors employed and details on their installation are described in the following subsections.

PRECAST PRESTRESSED GIRDERS

A total of 86 vibrating wire strain gauges (VWSG) with built-in thermistors (type EM-5) were used to monitor the strain and stress variations, as well as temperature changes in the PC/PS girders, and the RC deck from fabrication through service life.

A total of 62 VWSGs were installed in all spans within the PC/PS girders of lines 3 and 4 before casting. The PC/PS girder's cluster locations at which the VWSG were placed are illustrated in Fig. 2. Within each girder of span 1 and span 3, the instrumentation clusters

were located at two cross-sections. One section was located at mid-span, and the other section was placed at approximately 0.61 m (2 ft.) from the support centerline of bents 2 and 3. The instrumentation clusters for span 2 were arranged at three different cross-sections: one at the mid-span and two at approximately 0.61 m (2 ft.) from each support centerline.
Several details on VWSGs installed at the girders' near-support and mid-span sections before concrete was cast are illustrated in Fig. 3. The following notation was used to identify the layers at which the VWSG sensors were installed:

TD: Top deck [150 mm (6 in.) above the bottom fiber of deck]
BD: Bottom deck [50 mm (2 in.) above the bottom fiber of deck; mid-span only]
TF: Top flange [50 mm (2 in.) below its top fiber]
CGC: Center of gravity of composite beam section
CGU/CGI: Center of gravity of the non-composite beam section (mid-span only)
CGS: Center of gravity of prestressed strands
BF: Bottom flange [50 mm (2 in.) above the bottom fiber]

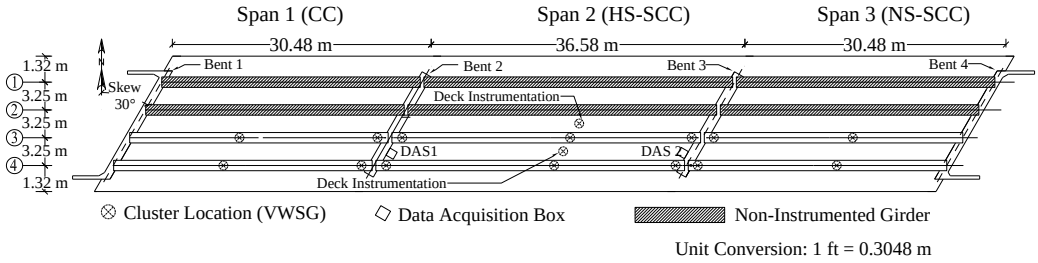

Fig. 2. Bridge A7957 instrumentation layout

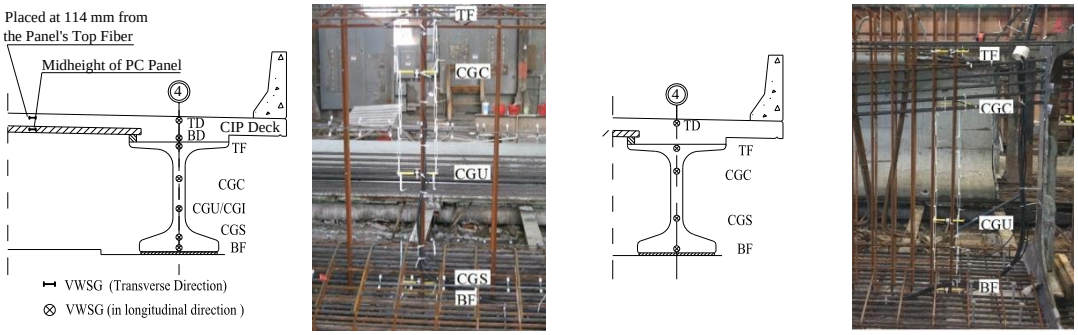

(a) Mid-span (b) Near support

Fig. 3. VWSG installation details (girders)

PRECAST PRESTRESSED PANELS AND CIP DECK

A VWSG was set at mid-height of two selected PC/PS panels [Fig. 4(a)]. The VWSGs installed within the CIP deck (mid-span sections) are illustrated in Fig. 4(b). Twenty two VWSGs were placed within the CIP RC deck. Twenty VWSGs were installed along the girder's longitudinal direction [Sensors TD and BD in Fig. 3 and Fig. 4(b)]. The last two VWSGs were set along the bridge's transverse direction between girder lines 2 and 3 and girder lines 3 and 4 [Fig. 2 and Fig. 3(a)]. These two VWSGs were placed directly above the

sensor that was installed within the panels, separated 114 mm (4.5 in.) from the panels' top fiber [Fig. 3(a)].

(a) PC/PS panels (b) CIP deck

Fig. 4. VWSG installation details (panels and deck)

FIELD LOAD TEST DESCRIPTION

An instrumentation program was planned and performed to monitor the girders response during the service life of Bridge A7957. The first part of the load tests was conducted in April, and the second part was performed in August of 2014. The following sections describe the load test procedure and load configurations planned to obtain the maximum response of the girders of each span.

LOAD TEST PROCEDURE

Six MoDOT H20 dump trucks were used to produce maximum load effects on the bridge superstructure during the live load test (days 1 and 2), and three dump trucks were employed on day 3 of the load test. The average trucks' dimensions are shown in Fig. 5. The trucks' weights (as reported by MoDOT personnel) are presented in Table 1.

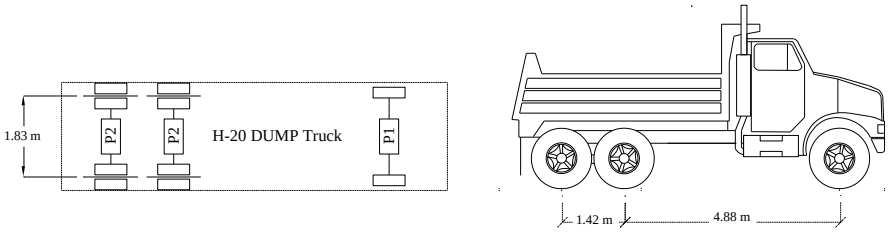

Fig. 5. Dump truck employed during field load test. P1 (front axle weight); P2 (total rear axles' weight). Conversion factor: 1 m = 3.28 ft.

LOAD TEST CONFIGURATION

Thirteen load stops are reported herein. For load stops 1-3, two lanes of trucks were driven from east towards west. The trucks were parked at the center of spans 3, 2 and 1, respectively [Fig. 6(a)-6(c)]. For stops 4-6, the trucks were turned around, driven from west to east, and located at the center of spans 1, 2, and 3, respectively. For these first 6 load stops, the center

of the trucks' exterior wheels was separated 3.25 m (10.67 ft.) from the safety barrier's edge as illustrated in Fig. 7(a).

Table 1. Truck weights (reported by MoDOT personnel)

Test Day	Date	Truck	Rear (KN)	Front (KN)	Total (KN)
1, 2*	4/21/2014	1	158.2	74.0	232.2
1, 2*	4/21/2014	2	161.6	57.2	218.8
1, 2*	4/21/2014	3	150.3	56.0	206.3
1, 2*	4/21/2014	4	178.0	75.3	253.3
1, 2*	4/21/2014	5	170.2	77.9	248.1
1, 2*	4/21/2014	6	166.4	71.6	238.0
3	8/11/2014	1	164.6	61.1	225.7
3	8/11/2014	2	180.3	70.8	251.1
3	8/11/2014	3	169.1	70.4	239.5

Notes: 1 KN = 0.2248 kip. * The trucks remained loaded with the same weight during days 1 and 2.

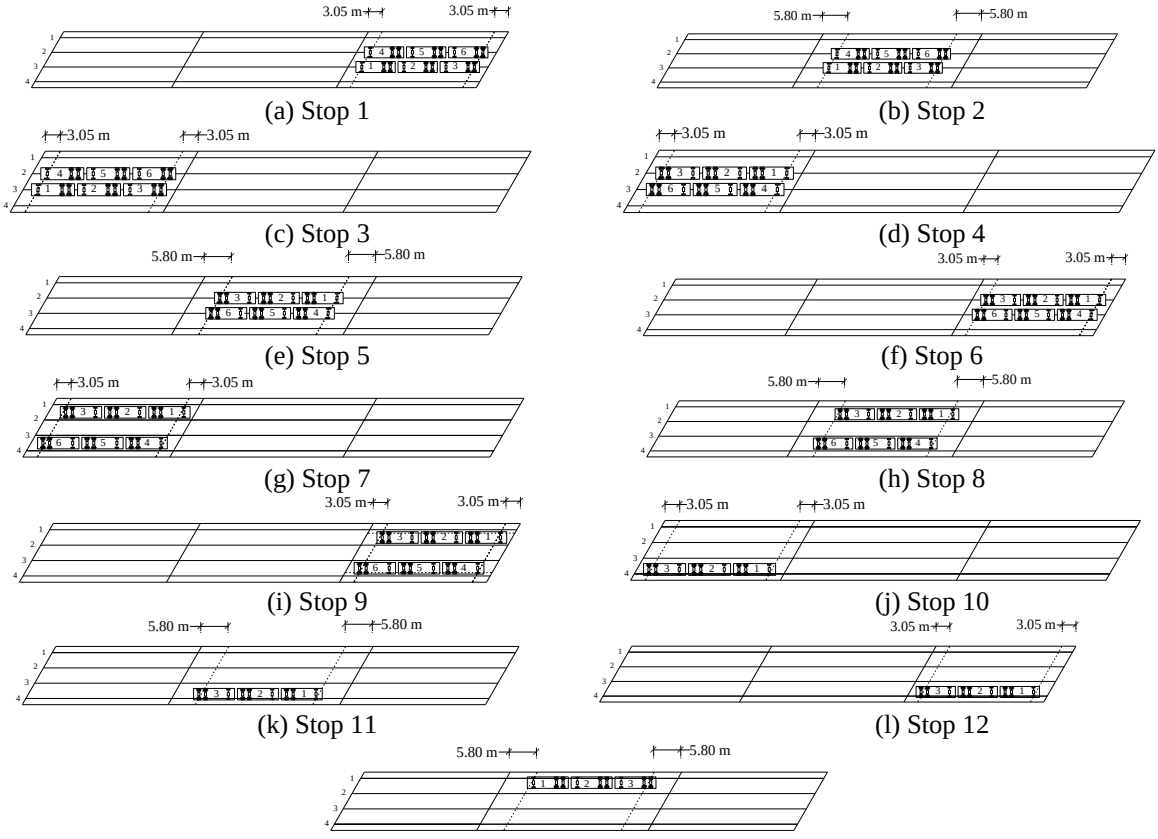

Fig. 6. Load test configurations (1 m = 3.28 ft.)

For stops 7-9, the trucks were driven from west to east as shown in Fig. 6(g)-6(i), and the

trucks' exterior axles were separated 0.60 m (2 ft.) from the barrier's edge [Fig. 7(b)]. These first nine stops are identified as two-lane load cases. For stops 10-12, a lane of three trucks was driven from west to east, and the trucks were separated 0.60 m (2 ft.) from the barrier's edge as illustrated in Fig. 7(c). The trucks remained parked within the central region of each span as shown in Fig. 6(j)-6(l) while measurements were recorded. Stop 13 consisted of a lane of three trucks parked on the north side of the central region of span 2, separated 0.60 m (2 ft.) from the safety barriers, as illustrated in Fig. 6(m) and Fig. 7(d).

LOAD TEST RESULTS

The girders' bottom flange strains for the first 13 load stops conducted on Bridge A7957 are presented in Table 2. These values correspond to the two-lane and one-lane load cases described on the previous section. Larger strains values were obtained at mid-span for the exterior and interior girders located in the vicinity of the applied load.

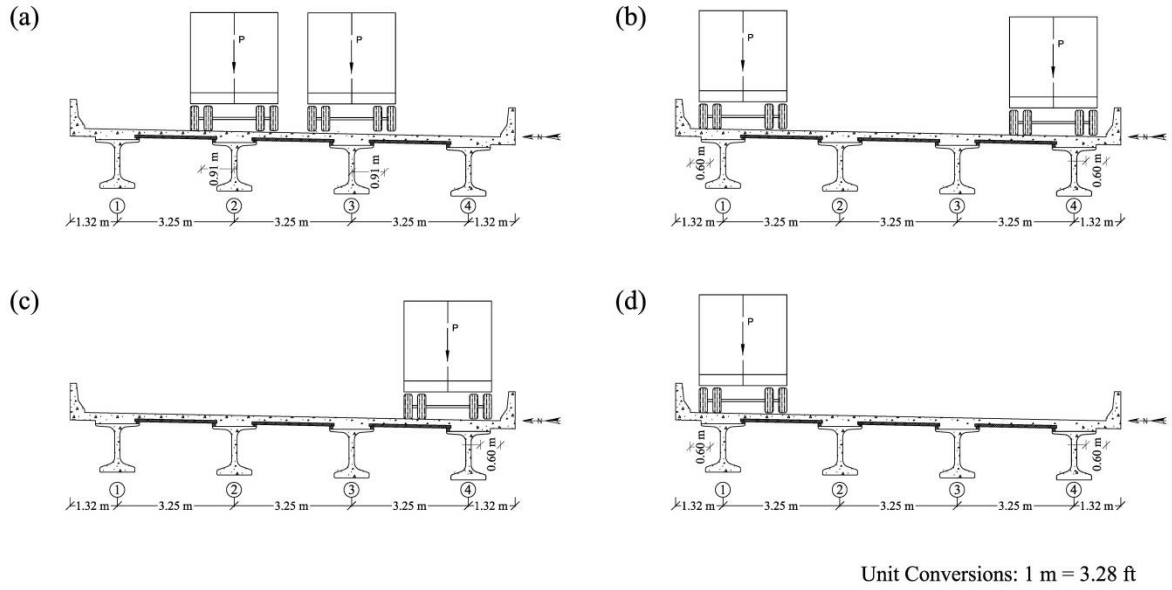

Fig. 7. Distance from trucks' exterior axle to barrier's edge: (a) Stops 1-6; (b) Stops 7-9; (c) Stops 10-12; (d) Stop 13

Measured strain values obtained from two-lane load stop configurations acting on spans 1 and 3 (i.e., stops 1 and 3, stops 4 and 6, and stops 7 and 9) were compared. No significant difference was observed in the service response of the exterior or interior girders of spans 1 and 3. In the case of load stops 10 and 12 (one-lane loaded cases), the difference in the strain values reported was closed to 10 percent. The difference in the results obtained may be attributed to two possible reasons. First, the trucks loading the bridge during load test stops 10 and 12 might have been placed at locations that are not symmetrical [according to Fig. 6(j) and 6(l)]. Second, the load test stop might have not lasted enough time to allow the bridge undergo the total expected deflection. Both sources will be investigated and controlled in the next series of load tests to be conducted on this bridge. However, from the cases of two

lane load configurations, it was observed that the flexural response of the spans was independent of the materials employed in the fabrication of the PC/PS girders, namely CC (span 1) and SCC (span 3).

LATERAL LOAD DISTRIBUTION

The distribution factors were obtained from field measurements and from the AASHTO LRFD approach[2]. The distribution factors computed from each approach were defined using the same nomenclature employed by Cai and Shahawy[4]. Distribution factors computed from field strain values measured at the bottom flange of the girders' (mid-span sections) were defined as load distribution factors (*LDF*ε). Distribution factors that were computed using the AASHTO LRFD method were referred to as girder distribution factors (*GDF*).

Table 2. Bottom flange strains, με

Stop (1)	Span (2)	ε_{G1}* (3)	ε_{G2}* (4)	ε_{G3}† (5)	ε_{G4}† (6)
Two Lanes Loaded					
3	1	46	84	87	49
4	1	49	87	84	46
7	1	—	—	73	65
2	2	55	95	92	54
5	2	54	92	95	55
8	2	—	—	80	75
1	3	45	83	89	48
6	3	48	89	83	45
9	3	—	—	67	58
One Lane Loaded					
10	1	—	—	44	64
11	2	4	17	51	78
13	2	78	51	17	4
12	3	—	—	43	65

Notes: * Values were estimated. † Values were measured directly.

LOAD DISTRIBUTION FACTORS

Strain values at the bottom of the PC/PS girders 1 and 2 were necessary to compute the *LDF*ε. As describe previously, VWSGs were installed at cluster locations along girder lines 3 and 4 (Fig. 2 and Fig. 3) which allowed to directly obtain girder 3 and 4's strains for each load stop. Girder 1 and 2's strains were indirectly obtained by considering the bridge's symmetry and assuming that mirrored image load stops could produce a symmetrical response of the interior and exterior girders 3 and 4 during the field load test. In the case of two lanes loaded, stops 3 and 4 (span 1), stops 2 and 5 (span 2), and stops 1 and 6 (span 3) were considered as symmetrical load stops. Stops 11 and 13 (span 2) were assumed as

mirrored load stops for the case of one lane loaded (Fig. 6). Stop 3 strains are reported in row 3 (Table 2). Girder 3 and 4's strains (reported in columns 5 and 6 of Table 2) were directly recorded from load stop 3. Girder 1 and 2's strains, as reported for stop 3 (columns 3 and 4 of Table 2), were interpreted from stop 4's measurements (recorded by sensors installed within girders 3 and 4). The same approach was employed to obtain the strains for the rest of the load stop configurations. Girder 1 and 2's strain values were not obtained for those load stops (stops 7-10 and 11) without a mirrored load stop image. The $LDF\varepsilon$ for interior and exterior girders from measured strains were computed with Eq. (1). Where $LDF\varepsilon_i$ = load distribution factor of ith girder; n = number of lanes loaded; ε_{maxi} = bottom flange strain (computed from field measurements) of the ith girder at mid-span; and k = number of girders.

$$LDF\varepsilon_i = \frac{n\varepsilon_{\max_i}}{\sum_{j=1}^{k}\varepsilon_{\max\, j}} \quad (1)$$

$LDF\varepsilon$ results are presented in Table 3. It is noted that there is no significance difference between the load distribution factors obtained from span 1 and 3's measurements. In addition, the interior girders' $LDF\varepsilon$ values obtained for one-lane load cases are similar to the results reported by Pantelides[6] in the case of a bridge built with PC/PS AASHTO Type IV girders and precast deck panels reinforced with GFRP bars. Furthermore, $LDF\varepsilon$ values presented in Table 3 are similar to values obtained from deflection measurements previously reported by Hernandez and Myers[7].

Table 3. Load Distribution Factors

Span	Stop	$LDF\varepsilon_{G1}$	$LDF\varepsilon_{G2}$	$LDF\varepsilon_{G3}$	$LDF\varepsilon_{G4}$
Two Lanes Loaded					
1	3	0346	0.632	**0.654**	**0.368**
1	4	**0.368**	**0.654**	0.632	0.346
2	2	**0.372**	**0.642**	0.622	0.365
2	5	0.365	0.622	**0.642**	**0.372**
3	1	0.340	0.626	**0.672**	**0.362**
3	6	**0.362**	**0.672**	0.626	0.340
One Lane Loaded					
2	11	0.027	0.113	**0.340**	**0.520**
2	13	**0.520**	**0.340**	0.113	0.027

GIRDER DISTRIBUTION FACTORS

The AASHTO LRFD[2] equations used to estimate the flexural GDF are presented in Table 4. Where S = girder spacing (mm); L = span length (mm); t_s = deck thickness (mm); K_g = stiffness parameter (mm^4); $K_g = n(I_g+e_g^2A_g)$; e_g = girder eccentricity (distance from the girder centroid to the middle centroid of the slab); E = modulus of elasticity of the concrete computed as $57{,}000\sqrt{f'c}$; n = modular ratio; I_g = girder moment of inertia (mm^4); A_g =girder area (mm^2); d_e = distance from exterior girder's centroid to barrier's edge (mm); θ, skew

angle; *SF*, skew correction factor (used if $30^o \leq \theta \leq 60^o$); m_p = multiple presence factor.

Table 4. AASHTO LRFD Flexural Girder Distribution Factors

Interior	Exterior
Two or More Design Lanes Loaded	
$GDF_{int}^{m} = 0.075 + \left(\frac{S}{2900}\right)^{0.4}\left(\frac{S}{L}\right)^{0.2}\left(\frac{K_g}{Lt_s^3}\right)^{0.1}$	$GDF_{ext}^{m} = \mathrm{e}\left(GDF_{int}^{m}\right)$ $\mathrm{e} = 0.77 + \frac{d_e}{2800} \geq 1$
One Design Lane Loaded	
$GDF_{int}^{s} = 0.06 + \left(\frac{S}{4300}\right)^{0.4}\left(\frac{S}{L}\right)^{0.3}\left(\frac{K_g}{Lt_s^3}\right)^{0.1}$	$GDF_{ext}^{s} = m_p\left(\frac{S + d_e - 1524}{S}\right)$ Lever rule

The variables used to compute the *GDFs* of Bridge A7957's spans are listed in Table 5. The *GDF* values computed for interior and exterior girders are presented in Table 6. The ASSHTO distribution factor equations listed in Table 4 implicitly include multiple presence factors which consider the most critical load scenario for a bridge. The simple static distribution approach, referred to as the "lever rule", was used to estimate the exterior girders' GDF when a single lane is loaded; a multiple presence factor was use in this case.

Table 5. Bridge A7957 Parameters to Estimate GDF (AASHTO LRFD Approach)

Variable	Span 1 = Span 3	Span 2
S, mm (ft.)	3250 (10.67)	3250 (10.67)
L, mm (ft.)	30480 (100.0)	36580 (120.0)
t_s, mm (in.)	240 (9.5)	240 (9.5)
f'_c, MPa (ksi)	55.2 (8.0)	58.9 (10.0)
$n=E_{beam}/E_{slab}$	1.41	1.58
A_g, mm^2 (in^2)	479.9x10^3 (743.9)	479.9x10^3 (743.9)
I_g, mm^4 (in^4)	1.2383x10^{11} (297512)	1.2383x10^{11} (297512)
e_g, mm (in.)	880 (34.7)	880 (34.7)
K_g, mm^4 (in^4)	702.207x10^9 (1686724)	785.936x10^9 (1885815)
θ, deg.	30	30
d_e, mm (ft)	914 (3.0)	914 (3.0)
C_1	0.1004	0.0901
SF	0.956	0.961

A skew factor was computed to reduce the AASHTO *GDF* values because Bridge A7957's skew angle is within the range of applicability of this correction factor (i.e., $30^o \leq \theta \leq 60^o$). For each span, the skew factors, *SF*, were computed with Eqs. (2) and (3).

$$SF = 1 - C_1(\tan\theta)^{1.5} \quad (2)$$

$$C_1 = 0.25\left(\frac{K_g}{L.t_s^{\,3}}\right)^{0.25}\left(\frac{S}{L}\right)^{0.5} \quad (3)$$

Table 6. Computed GDF (AASHTO LRFD)

Span	Case	GDF_{int}	GDF_{int} (corrected)	GDF_{ext}	GDF_{ext} (corrected)
1, 3	2 or more lanes loaded	0.819	0.783	0.901	0.861
1, 3	1 lane loaded	0.558	0.533	0.975	0.932
2	2 or more lanes loaded	0.788	0.756	0.866	0.832
2	1 lane loaded	0.528	0.507	0.975	0.936

RESULTS AND DISCUSSION

By definition, the load distribution factor (LDF) and girder distribution factor (GDF) correspond to the maximum value obtained for the interior and exterior girders considering the most critical load cases producing the maximum effects on the girders. The value of the interior load distribution factor, LDF_{int}, and exterior load distribution factor, LDF_{ext}, were 0.672 and 0.520, respectively. The computed AASHTO LRFD interior girder distribution factor, GDF_{int}, was 0.783, and the exterior girder distribution factor, GDF_{ext}, was 0.936. These results reflect that AASHTO girder distribution factors are larger and more conservative than the load distribution factors obtained from field measurements. It is important to mention that the AASHTO LRFD provides a methodology that is used for designing highway bridges. The AASHTO LRFD approach does not intent to evaluate the load distribution response of existing bridge structures for which a diagnostic field load test would be more suitable.

CONCLUSIONS

The first full-scale structure implementation of high-strength self-consolidating concrete (HS-SCC) and high volume fly ash concrete (HVFAC) has been implemented on the structure of Bridge A7957 through the Missouri Department of Transportation (MoDOT).

The first series of live load tests was conducted on Bridge A7957 to monitor its initial in-service flexural response. In general, the in-service response of the SCC and CC PC/PS girders was similar which implies that the in-service response should not hinder the use of SCC in future bridge project implementations.

Load distribution factors are critical in the design of new bridges and in the serviceability assessment of existing bridges. Load distribution factors (*LDF*) were obtained from field test

measurements, and girder distribution factors (*GDF*) were obtained using the AASHTO LRFD approach. The AASHTO *GDFs* resulted in larger values compared to the experimental LDF values. Reasons that explain the variability between the lateral load distribution values obtained from each method may be attributed to several factors. The AASHTO LRFD equations were developed to be applied to different type of bridges, with a wide range of span lengths, girders' spacing and stiffness. LDFs which are obtained from field load tests implicitly take into account in-situ parameters such as unintended support constraints and continuity, skew angle, contribution of secondary members, and multiple presence factors which can contribute to improve the bridge's in-service behavior. More research should be conducted to evaluate such differences and the cases of applicability of each approach.

ACNOWLEDGEMENTS

The authors gratefully acknowledge the financial support provided by the Missouri Department of Transportation (MoDOT) and the National University Transportation Center (NUTC) at Missouri University of Science and Technology.

REFERENCES

1. Myers, J.J., Volz, J.S., Sells, E., Porterfield, K., Looney, T., Tucker, B., Holman, K., (2012) "Self-Consolidating Concrete (SCC) for Infrastructure Elements: Report A – Shear Characteristics," Final Report A MoDOT TRyy1103, Missouri Department of Transportation, Jefferson City, Missouri, August, 2012, 237 pp.
2. American Association of State Highway and Transportation Officials (2012). "AASHTO LRFD Bridge Design Specifications, 6th Edition." *American Association of State Highway and Transportation Officials*. Washington (DC).
3. Barker, R.M., Pucket, J.A., *Design of Highway Bridges: An LRFD Approach. 3rd Edition*. John Wiley & Son. Hoboken, New Jersey, 2013.
4. Cai, C.S., Shahawy, M., Understanding Capacity Rating of Bridges from Load Tests. *ASCE Practice Periodical on Structural Design and Construction. 8(4), 209-216.* November, 2003.
5. Hernandez, E.S., Griffin, A., Myers, J.J., Balancing Extended Service Life and Sustainable Concrete Usage in Missouri Bridge A7957, *2014 Structural Faults & Repair: European Bridge Conference (SF&R 2014)*, 9 pages, London, England, UK, July 8-10, 2014.
6. Pantelides, C.P., Ries, J., Mix, R., Construction and Monitoring of a Single-Span Bridge with Precast Concrete Glass-Fiber-Reinforced Polymer Deck Panels. *PCI Journal, 58(1), 78-94.* Winter, 2013.
7. Hernandez, E., Myers, J., In-Situ Field Test and Service Response of Missouri Bridge A7957, *16th European Bridge Conference*, 10 pages, Edinburg, Scotland, June 23-25, 2015.